AGU PUBLICATIONS

Paleoceanography

RESEARCH ARTICLE
10.1002/2014PA002729

Key Points:
- Bottom water redox changes triggered carbon burial within the WIS during OAE 3
- Anoxia developed due to O_2 drawdown in a stratified water column
- Redox-controlled changes in OM preservation altered primary δ^{13}Corg signals

Supporting Information:
- Figures S1 and S2

Correspondence to:
A. Tessin,
atessin@umich.edu

Citation:
Tessin, A., I. Hendy, N. Sheldon, and B. Sageman (2015), Redox-controlled preservation of organic matter during "OAE 3" within the Western Interior Seaway, *Paleoceanography*, *30*, 702–717, doi:10.1002/2014PA002729.

Received 26 SEP 2014
Accepted 14 MAY 2015
Accepted article online 19 MAY 2015
Published online 16 JUN 2015

©2015. American Geophysical Union. All Rights Reserved.

Redox-controlled preservation of organic matter during "OAE 3" within the Western Interior Seaway

Allyson Tessin[1], Ingrid Hendy[1], Nathan Sheldon[1], and Bradley Sageman[2]

[1]Department of Earth and Environmental Sciences, University of Michigan, Ann Arbor, Michigan, USA, [2]Department of Earth and Planetary Sciences, Northwestern University, Evanston, Illinois, USA

Abstract During the Cretaceous, widespread black shale deposition occurred during a series of Oceanic Anoxic Events (OAEs). Multiple processes are known to control the deposition of marine black shales, including changes in primary productivity, organic matter preservation, and dilution. OAEs offer an opportunity to evaluate the relative roles of these forcing factors. The youngest of these events—the Coniacian to Santonian OAE 3—resulted in a prolonged organic carbon burial event in shallow and restricted marine environments including the Western Interior Seaway. New high-resolution isotope, organic, and trace metal records from the latest Turonian to early Santonian Niobrara Formation are used to characterize the amount and composition of organic matter preserved, as well as the geochemical conditions under which it accumulated. Redox sensitive metals (Mo, Mn, and Re) indicate a gradual drawdown of oxygen leading into the abrupt onset of organic carbon-rich (up to 8%) deposition. High Hydrogen Indices (HI) and organic carbon to total nitrogen ratios (C:N) demonstrate that the elemental composition of preserved marine organic matter is distinct under different redox conditions. Local changes in δ^{13}C indicate that redox-controlled early diagenesis can also significantly alter $\delta^{13}C_{org}$ records. These results demonstrate that the development of anoxia is of primary importance in triggering the prolonged carbon burial in the Niobrara Formation. Sea level reconstructions, δ^{18}O results, and Mo/total organic carbon ratios suggest that stratification and enhanced bottom water restriction caused the drawdown of bottom water oxygen. Increased nutrients from benthic regeneration and/or continental runoff may have sustained primary productivity.

1. Introduction

Over the many years of research on black shale deposition, a primary goal has been identification of the key mechanism(s) responsible for organic matter burial rates sufficient to produce these important facies. As with so many other issues, the tendency to dichotomize has been attractive, and thus, following the seminal work of *Demaison and Moore* [1980] and *Pedersen and Calvert* [1990] on organic-rich sedimentation, "production versus preservation" dominated the discussion for many years. More recent efforts to develop a comprehensive model have argued that at least three major factors play key roles in the development of organic carbon-rich black shales: rate of export production, rate of organic matter decomposition during early burial (in particular, oxygen exposure time) [*Hartnett et al.*, 1998], and rate of organic matter dilution by other sedimentary materials [e.g., *Sageman and Lyons*, 2003; *Bohacs et al.*, 2005; *Sageman et al.*, 2014]. Together, these factors likely account for most organic matter burial in marine and lacustrine deposits, although there may be variations in the relative contribution of each, and in some cases additional influences, such as mineral surface area, may play a contributing role [e.g., *Kennedy et al.*, 2002; *Kennedy and Wagner*, 2011]. Nonetheless, reduced benthic oxygen levels, whether a consequence of hydrographic factors such as water column stratification or enhanced consumption due to extreme export production, appear to be a consistent feature.

Mesozoic ocean anoxic events, the canonical examples of oxygen depletion and massive organic matter accumulation, were first defined almost 40 years ago, when black shales were discovered in stratigraphic intervals of deep-sea cores suggesting widespread anoxic deposition in the marine realm [*Schlanger and Jenkyns*, 1976]. Although only two of the designated Mesozoic Oceanic Anoxic Events (OAEs) have proven to be consistently expressed globally (OAE 1a and OAE 2), the term has been applied to as many as nine intervals during the Late Jurassic to early Cenozoic [*Jenkyns*, 2010]. Because the individual events differ in duration, expression, and geographic extent, most likely because they are triggered by different environmental conditions and depositional mechanisms, they offer an opportunity to deconvolve the relative roles of these forcing factors more effectively.

Coniacian-Santonian-age black shales represent one of the nonglobal OAEs, termed OAE 3 [e.g., *Locklair et al.*, 2011; *Wagreich*, 2012]. It is unlike the quintessential Cenomanian-Turonian boundary event (C-T OAE 2), which is clearly defined by black shales in many localities [*Schlanger et al.*, 1987; *Tsikos et al.*, 2004], and has a distinctive and relatively short lived (~600 ka) [*Sageman et al.*, 2006] positive carbon isotope excursion that is expressed almost everywhere in the world that C-T deposits are preserved [*Arthur et al.*, 1987; *Jenkyns*, 2010]. In contrast, organic carbon-rich sedimentation during OAE 3 was restricted to the equatorial Atlantic and adjacent continental shelves and seaways [e.g., *Hofmann et al.*, 2003; *Wagner et al.*, 2004; *Beckmann et al.*, 2005; *Marz et al.*, 2008; *Locklair et al.*, 2011], including the North American Western Interior Seaway (WIS), with an absence of significant black shale deposition in the Tethys and Pacific basins [*Arthur and Sageman*, 1994; *Jenkyns*, 2010; *Wagreich*, 2012]. In localities where Coniacian-Santonian organic-rich strata have been found, the age and duration of carbon burial varies considerably, further complicating the identification of the event [*Locklair et al.*, 2011]. In some regions, including the WIS, organic carbon burial rates were roughly double that of OAE 2 and carbon burial persisted for a significantly longer duration ($>$3 Myr), indicating that despite the lack of global organic carbon burial, OAE 3 represents a significant carbon cycle perturbation [*Locklair et al.*, 2011; *Wagreich*, 2012]. While the triggering mechanisms and feedbacks of short-lived, near-global OAEs, such as OAE 2, have become increasingly well understood [e.g., *Turgeon and Creaser*, 2008; *Du Vivier et al.*, 2014], the prolonged period of carbon burial within the WIS during the Coniacian-Santonian requires different depositional mechanisms. Under modern climatic conditions, organic carbon burial in similar shallow marine environments plays an important role in the global carbon cycle with $>$40% of marine organic carbon sequestration occurring on continental margins [*Muller-Karger et al.*, 2005]. Therefore, while Coniacian-Santonian carbon burial may not manifest in the rock record as an OAE sensu stricto, a better understanding of such regional shallow marine carbon burial events has important implications for predicting how carbon burial in shallow marine settings may change in response to anthropogenically driven expansion of low-oxygen marine environments in response to future warming and marine eutrophication.

A better understanding of the extended period of Coniacian-Santonian black shale deposition and the role that oxygenation played requires regional records of carbon burial and redox history. Here we present high-resolution isotope, organic and trace metal records from the latest Turonian to early Santonian Niobrara Formation of the WIS to help characterize the amount and composition of organic matter preserved in the region, as well as the geochemical conditions under which it accumulated. These results allow for the evaluation of redox-controlled preservation as a potential mechanism for regional organic carbon-rich deposition in the WIS and a possible mechanism for black shales deposited in other regions and at other times.

2. Background

2.1. Geologic Setting

During Cretaceous peak highstand intervals, the WIS flooded the North American continental interior, linking the northern Boreal Sea with the Tethys Ocean to the south (Figure 1). The WIS formed due to glacio- and tectono-eustatic forces, as well as accommodation space created by the subsidence of a retroarc foreland related to crustal loading of the Sevier Orogenic Belt to the west [*Kauffman and Caldwell*, 1993]. The record of the WIS includes episodic deposition of organic carbon-rich shales and chalks, including those recorded during the two maximum transgressions of the Greenhorn and Niobrara cyclothems [*Kauffman*, 1977]. The seaway had two main sources of water: warm, saltier Tethyan waters from the south and cooler, lower salinity Boreal waters from the north [e.g., *Hay et al.*, 1993; *Fisher et al.*, 1994]. Continental runoff from the Sevier Highlands delivered freshwater and nutrients to the seaway [e.g., *Floegel et al.*, 2005].

The Niobrara Formation was deposited in an asymmetrical foreland basin from the Late Turonian to the Early Campanian [*Scott and Cobban*, 1964; *Locklair and Sageman*, 2008] and is formally divided into two members: the basal Fort Hays Limestone and the overlying Smoky Hill Chalk (Figure 2). The late Turonian-early Coniacian Fort Hays Limestone consists of ledge-forming limestone beds separated by thin organic carbon-rich shales [*Scott and Cobban*, 1964]. The Smoky Hill Chalk consists of interbedded shales and chalks that *Scott and Cobban* [1964] divided into seven informal units (Figure 2).

Previous research on the Niobrara Formation illustrates the difficulty in identifying a single distinct carbon burial event during the Coniacian-Santonian associated with OAE 3, as there are several periods of

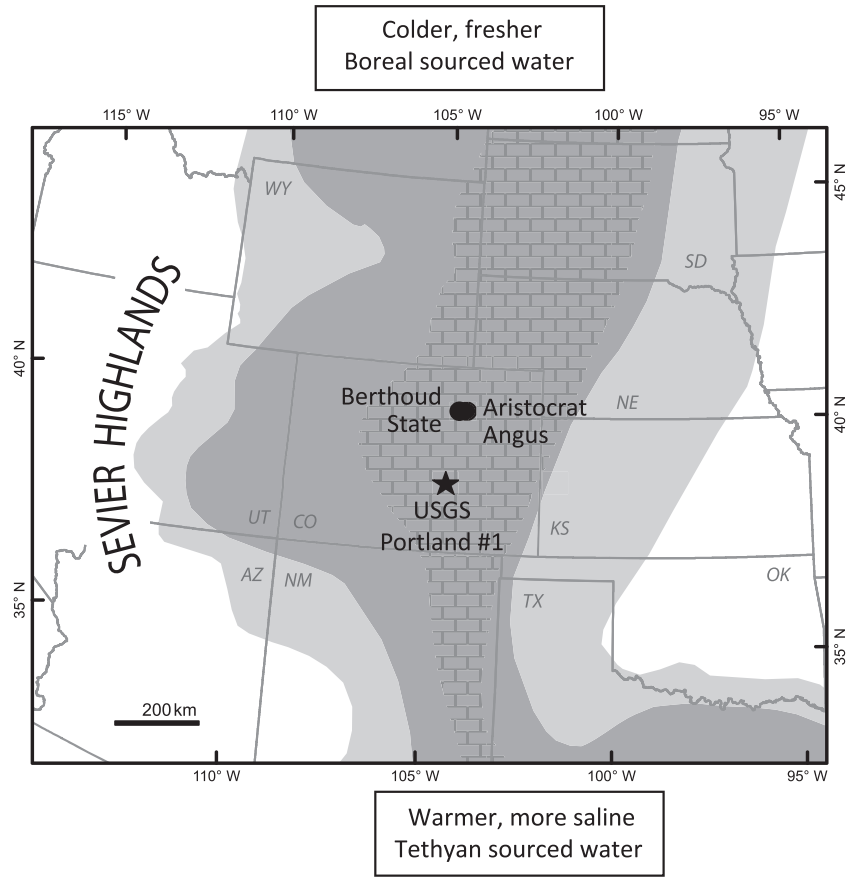

Figure 1. Map of the Cretaceous Western Interior Seaway (WIS) with Coniacian-Santonian paleogeography (adapted from *Roberts and Kirschbaum* [1995]). Dark gray represents marine shales and limestones, light gray represents the coastal plain, and white represents the alluvial plain. The USGS #1 Portland core location is marked with a star. The Berthoud State #3 and Aristocrat Angus cores are marked with circles. The Sevier Highlands are labeled to the west, and the major water sources are indicated to the north and south of the WIS.

elevated organic carbon burial [*Pratt et al.*, 1993; *Locklair et al.*, 2011]. *Locklair et al.* [2011] define three possible "OAE 3 intervals" during the middle Coniacian, the early Santonian, and at the Santonian-Campanian boundary. They assign the main OAE 3 interval to the middle Coniacian section, and this designation has been used in subsequent work [*Locklair et al.*, 2011; *Joo and Sageman*, 2014]. OAEs are traditionally defined by significant positive global carbon isotope excursions (>2‰) [*Jenkyns*, 2010]; however, records defined as the main OAE 3 interval from the WIS and elsewhere correspond to a comparatively small (<1‰) isotope excursion [*Pratt et al.*, 1993; *Jarvis et al.*, 2006; *Locklair et al.*, 2011]. For these reasons, the OAE 3 designation has been debated in the literature.

2.2. Trace Metal Geochemistry

Trace metal geochemistry has been used to study the mechanisms and characteristics of organic carbon burial in modern and paleo-environments [e.g., *Calvert and Pedersen*, 1993; *Brumsack*, 2006]. Molybdenum, Re, and Mn accumulate in sediments under variable redox conditions and can be used to identify differences in benthic oxygenation throughout the WIS records. Molybdenum accumulates in reducing sediments in the presence of free H_2S above a threshold concentration [*Helz et al.*, 1996]. Molybdenum concentrations enriched over background concentrations, but less than 25 ppm indicate the presence of pore water sulfide, while concentrations of greater than 100 ppm are interpreted as evidence for abundant water column sulfide. Concentrations between 25 and 100 likely indicate intermittent to persistent euxinia [*Scott and Lyons*, 2012]. Rhenium also accumulates in reducing sediments but unlike Mo, sedimentary enrichment does not require the presence of H_2S [*Crusius et al.*, 1996; *Morford et al.*, 2001]. As opposed to

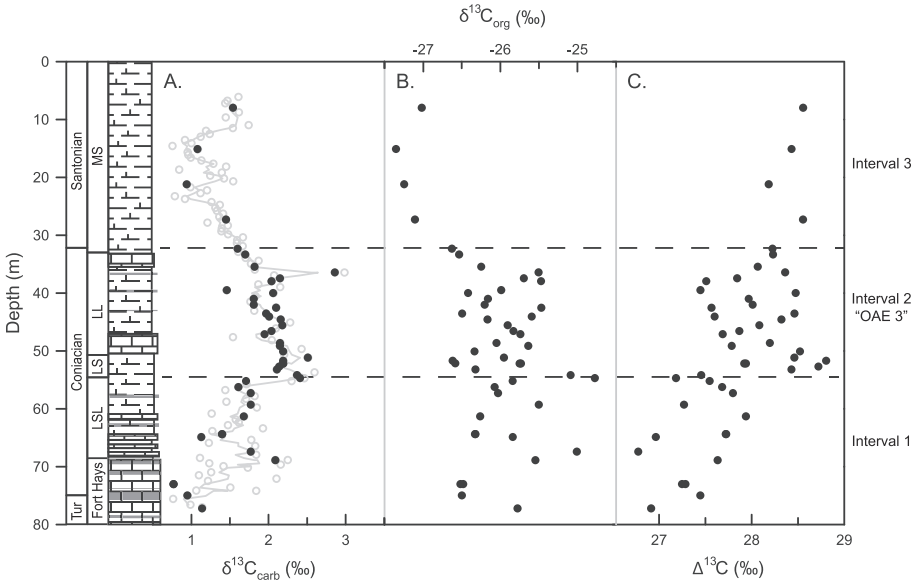

Figure 2. Stratigraphy and carbon isotope results from the USGS #1 Portland core. Lithostratigraphy was adapted from *Dean and Arthur* [1998]. $\delta^{13}C_{carb}$, $\delta^{13}C_{org}$, and $\Delta^{13}C$ records are plotted. $\delta^{13}C_{carb}$ records are plotted as gray circles with a three-point running average plotted as a gray line. The black symbols correspond to samples with $\delta^{13}C_{org}$ and $\Delta^{13}C$ measurements. Dashed lines designate the three intervals studied. Interval 2 corresponds to Ocean Anoxic Event (OAE) 3 as defined by *Locklair et al.* [2011].

the other metals discussed here, Mn is soluble in reducing waters as Mn^{2+}, which results in sedimentary Mn depletion in reducing environments, with the exception of settings in which Mn carbonates are formed [*Hild and Brumsack*, 1998]. Rhenium and Mo are enriched in reducing sediments and should be precipitated in sediments at different reduction potentials [*Crusius et al.*, 1996]. In oxic settings, the Re/Mo ratio will be low due to the low crustal ratio of Re/Mo. In suboxic settings, the Re/Mo ratio will be very high, due to large Re enrichments and little to no Mo enrichment. In more reducing settings, the Re/Mo ratio will be the seawater ratio, as both Re and Mo are removed from seawater [*Crusius et al.*, 1996]. Ratios of $>9\,\mathrm{mmol\,mol^{-1}}$ indicate suboxic conditions, while ratios of $<9\,\mathrm{mmol\,mol^{-1}}$ indicate anoxic conditions [*Crusius et al.*, 1996]. Thus, taken together, the suite of Mo, Re, and Mn can be used to differentiate between oxidizing and reducing and sulfidic and nonsulfidic conditions.

3. Methods and Materials

The Niobrara Formation within the U.S. Geological Survey (USGS) #1 Portland core was sampled at 0.5 m resolution at the USGS Core Research Center in Denver, Colorado (Figure 1). The Portland core was drilled and continuously cored in the Cañon City Basin, Colorado, where Cretaceous strata, including half of the Niobrara Formation, were collected [*Dean and Arthur*, 1998].

Bulk carbonate stable isotopes analyses were run on a Thermo Finnigan MAT 253 triple-collector gas source mass spectrometer coupled to a Finnegan Kiel automated carbonate device at the University of Michigan's Stable Isotope Laboratory. Isotope values were corrected to Vienna Peedee belemnite using National Bureau of Standards 19 ($n=32$, $\delta^{18}O=-2.18\pm0.07$‰, $\delta^{13}C=1.98\pm0.07$‰). Samples were reproduced with average standard deviations of 0.11‰ and 0.07‰, respectively. Organic carbon isotope analyses were run on a Delta V Plus mass spectrometer at the University of Michigan's Stable Isotope Laboratory. International Atomic Energy Agency (IAEA) 600 caffeine ($n=9$, $\delta^{13}C=-27.77\pm0.04$‰) and IAEA-CH-6 sucrose ($n=9$, $\delta^{13}C=-10.45\pm0.05$‰) standards were used to verify isotopic values. $\Delta^{13}C$ values were calculated as

$$\Delta^{13}C = \delta^{13}C_{carb} - \delta^{13}C_{org} \quad (1)$$

Carbon and nitrogen concentrations were measured on a Costech ECS4010 elemental analyzer. Total organic and inorganic carbon were determined using paired acidified (organic) and unacidified (total) carbon measurements. In preparation for analysis of total organic carbon, samples were acidified in 7% HCl until

all carbonate was removed. Dried samples were homogenized and loaded in tin capsules. Acetanilide standards were used to verify concentrations ($n = 48$, %C = 10.21 ± 0.05, %N = 71.37 ± 0.15), and 20% of sample concentrations were replicated. Replicates were reproduced with average standard deviations of 0.13% and 0.05%.

Rock-Eval pyrolysis analyses were performed at a commercial laboratory [*Espitalie et al.*, 1977; *Locklair*, 2007]. Hydrogen index (HI) is calculated as (S_2*100)/total organic carbon (TOC) where S_2 equals the amount of hydrocarbons produced through thermal cracking of nonvolatile organic matter in milligram hydrocarbons/g of rock. Oxygen index is calculated as S_3/TOC where S_3 is the amount of CO_2 produced during pyrolysis of kerogen in milligram CO_2/g of rock.

Samples for major and trace element geochemistry were ground to <75 μm and homogenized in an alumina shatterbox to minimize trace element contamination. Elemental analysis was completed on samples from the Portland core at ALS Laboratories in Vancouver, British Columbia. Whole rock samples were digested with perchloric, hydrofluoric, nitric, and hydrochloric acids. Concentrations were determined by inductively coupled plasma (ICP)-atomic emission spectroscopy and inductively coupled plasma (ICP)-mass spectroscopy GRM908, OREAS 90 and MRGeo08 standards were used to verify elemental concentrations. Sample replicates reproduced with average standard deviations are as follows: Al = 0.09%, Mn = 11 ppm, Mo = 0.21 ppm, and Re = 0.007 ppm.

Trace metal records are presented as excess concentrations, which are calculated as follows:

$$TM_{xs} = TM_{sample} - Al_{sample}\left(\frac{TM}{Al}\right)_{crustal} \quad (2)$$

where TM is the trace metal in question and Al is aluminum content. Excess concentrations are used to determine the nonlithogenic concentration of elements of interest and to compare between intervals of the core with distinctly different aluminum concentrations. This normalization is used rather than a simple ratio or enrichment factor because many of the elements studied herein have low crustal concentrations and large changes in aluminum could lead to overestimates of the change in metal enrichment [*Taylor and McLennan*, 1985; *McLennan*, 2001].

4. Results

4.1. Stratigraphy

Portland core stratigraphy is plotted in Figure 2. The Portland core includes the basal Fort Hays Limestone Member (FHL) and the lower shale and limestone (lsl), lower shale (ls), lower limestone (ll), and middle shale (ms) units of the Smoky Hill Chalk Member [*Scott and Cobban*, 1964]. Turonian, Coniacian, and Santonian boundaries are assigned based on comparison to the recent integrated astrochronological and radioisotopic age model of *Sageman et al.* [2014]. The Portland core is correlated to the Niobrara chronology using analogous lithostratigraphic units. Several possible diastems, including one at the top of the lower shale and limestone unit (Figure 2), have been identified in the Niobrara outcrops in Pueblo, Colorado, based on biostratigraphic data [*Walaszczyk and Cobban*, 2000, 2006, 2007]. Recent astrochronological work [*Locklair and Sageman*, 2008] did not indicate evidence of hiatuses, but some were later identified by biostratigraphy [*Walaszczyk et al.*, 2014], reflecting the fact that it is possible for hiatuses with certain characteristics to remain undetected by spectral methods [*Meyers and Sageman*, 2004]. Based on comparison of radioisotopically and astrochronologically derived durations spanning the proposed hiatuses of the lower Niobrara Formation, *Sageman et al.* [2014] concluded that their duration did not exceed 0.5 million years. If short-term hiatuses were present, the geochemical record of transitions between units would likely be sharper than the transitions actually were, but this should not alter the overall conclusions presented in this paper.

For the following discussion, three intervals are assigned based on geochemical results. In the Portland core, Interval 1 includes the FHL and the lsl member of the Smoky Hill (Figure 2). This unit is defined as the period before the OAE 3 positive carbon isotope plateau. Based on correlation to radioisotopically dated sections, this interval spans the latest Turonian to the middle Coniacian. Interval 2 is defined as the OAE 3 positive isotope plateau and corresponds to an OAE 3 interval defined by *Locklair et al.* [2011]. In the Portland core, this corresponds to the ls and ll units of the Smoky Hill. This interval was deposited during the middle to

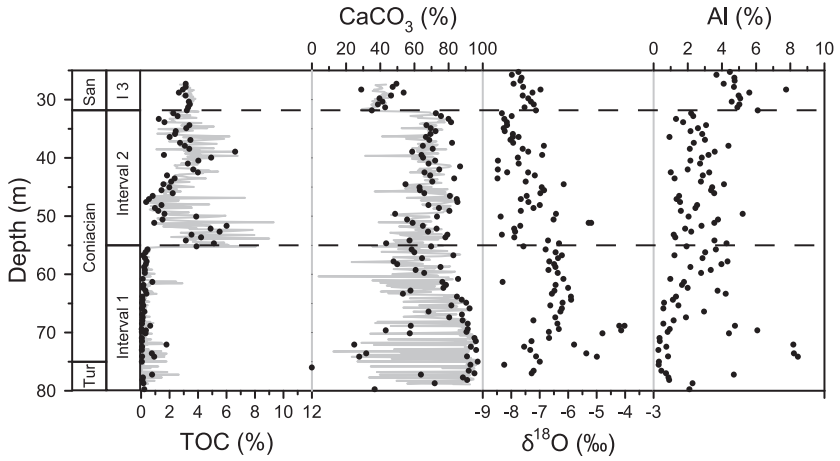

Figure 3. Total organic carbon, carbonate, $\delta^{18}O$, and aluminum for the Portland core are plotted. High-resolution organic carbon and carbonate data from *Locklair et al.* [2011] for the Portland core are plotted in gray, and new results are plotted in black. Dashed lines indicate the correlated intervals.

late Coniacian. While not the focus of this paper, Interval 3 is defined by the lower $\delta^{13}C$ values recorded after the OAE 3 isotope plateau and was deposited during the Santonian. In the Portland core, Interval 3 includes the middle shale unit of the Smoky Hill (Figure 2).

4.2. Bulk Carbonate and Organic $\delta^{13}C$

Bulk carbonate and organic $\delta^{13}C$ results on the Portland core are plotted in Figure 2. Bulk $\delta^{13}C_{carb}$ values increase by ~2‰ from the base of the Niobrara Formation during Interval 1. This isotope excursion occurs in two steps with $\delta^{13}C_{carb}$ increasing throughout the Fort Hays Limestone and again leading into Interval 2. $\delta^{13}C_{carb}$ values then decrease through the Coniacian-Santonian boundary with 0.5 to 1‰ positive excursions occurring at 45 and 35 m.

Bulk $\delta^{13}C_{org}$ values range between −26.6 and −27.8‰ during Intervals 1 and 2. Short-term positive excursions at 67 and 55 m, similar to those recorded in the carbonate record, are found in the $\delta^{13}C_{org}$. During Interval 3, $\delta^{13}C_{org}$ values decrease to an average of −27.1‰ (Figure 2). During Interval 1, $\Delta^{13}C$ values range between 26.8 and 27.9‰ with a generally increasing trend from the base to the onset of Interval 2. Above 50 m, $\Delta^{13}C$ values are consistently greater than 27.5‰ with values as high as 28.8‰.

4.3. TOC, $CaCO_3$, Al, and $\delta^{18}O$

Total organic carbon (TOC), carbonate ($CaCO_3$), aluminum (Al), and $\delta^{18}O$ records for the Portland core are plotted in Figure 3. The new TOC results are generally consistent with previously published high-resolution data from *Locklair et al.* [2011]. Interval 1 corresponds to relatively low TOC concentrations, generally less than 0.5%, with higher values representing thin shale interbeds (Figure 3). TOC increases dramatically in both cores during Interval 2. TOC concentrations during Interval 2 are characterized by two periods of TOC values >5% from 55 to 50 m and 42 to 34 m with lower concentrations in between.

In general, Al and $CaCO_3$ concentrations inversely covary (Figure 3). Al concentrations increase during the second half of Interval 1 and remain relatively constant throughout Interval 2 before increasing dramatically at the base of Interval 3. Intervals 1 and 2 are associated with an average $CaCO_3$ concentration of 71%. A distinct drop in the $CaCO_3$ concentration occurs at the base of Interval 3, with $CaCO_3$ concentrations averaging 39%. The greatest variability in Al and $CaCO_3$ concentrations occurs during Interval 1 and is a product of the highly variable lithology found in the FHL. The characteristic rhythmic bedding within the FHL that produces variable limestone and organic-rich clay interbeds has been interpreted as either changes in dilution by riverine input or changes in carbonate productivity [i.e., *Dean and Arthur*, 1998; *Locklair and Sageman*, 2008]. Values of $\delta^{18}O$ in the Portland core range from −4 to −8.5‰. Significant variability exists within the first half of Interval 1, which records the cyclic deposition of the Fort Hays. Generally, the highest values are recorded in the middle of Interval 1 with generally lower values throughout Interval 2. The average $\delta^{18}O$ values recorded during Interval 1 and Intervals 2 and 3 are −6.39‰ and 7.48‰, respectively.

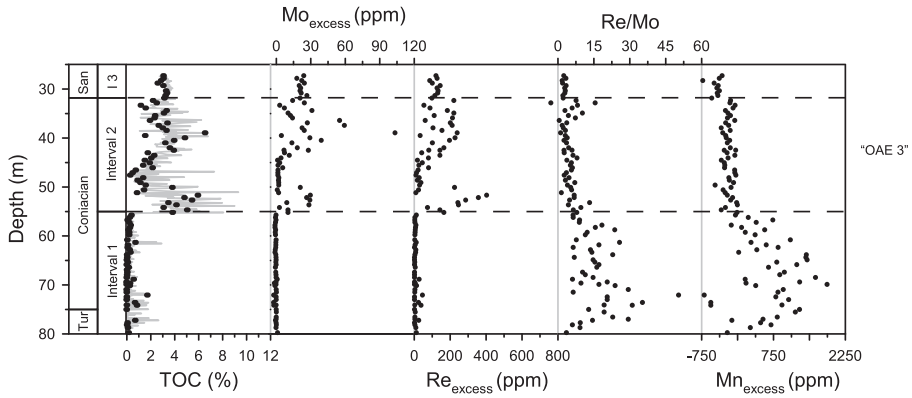

Figure 4. Excess concentrations of redox sensitive trace metals (Re, Mo, Re/Mo, and Mn) plotted with total organic carbon from the Portland core. High-resolution organic carbon data from *Locklair et al.* [2011] for the Portland core are plotted as gray lines, and new results that are paired with trace metal concentrations are plotted as black dots. Dashed lines indicate the correlated intervals.

4.4. Redox Sensitive Metals

Records of Mo and Re excess concentrations exhibit patterns that generally covary with the TOC record (Figure 4). During Interval 1, Mo and Re excess concentrations are relatively low (less than 0.5 ppm and 5 ppb, respectively). Excess concentrations of both Mo and Re increase dramatically at the base of Interval 2, with maximum excess concentrations of ~100 ppm and ~450 ppb, respectively. Mo and Re excess concentrations track TOC during Interval 2, during which low TOC concentrations between 51 and 45 m correspond to excess concentrations similar to those found in Interval 1. At the base of Interval 3, Mo and Re excess concentrations decrease to intermediate values of ~20 ppm and ~120 ppb.

Re/Mo values and Mn excess concentrations trend opposite to those of Mo and Re excess concentrations (Figure 4). During Interval 1, Re/Mo values are generally >9 mmol mol^{-1}. Values increase from the base of Interval 1 to 72 m before decreasing to the base of Interval 2. Throughout the rest of the records, Re/Mo values are consistently <9 mmol mol^{-1}. Manganese excess concentrations increase from the base of Interval 1 to 70 m reaching maximum values of ~1900 ppm. Manganese excess concentrations then decrease throughout the rest of Interval 1 and remain <0 ppm throughout the rest of the record (Figure 4).

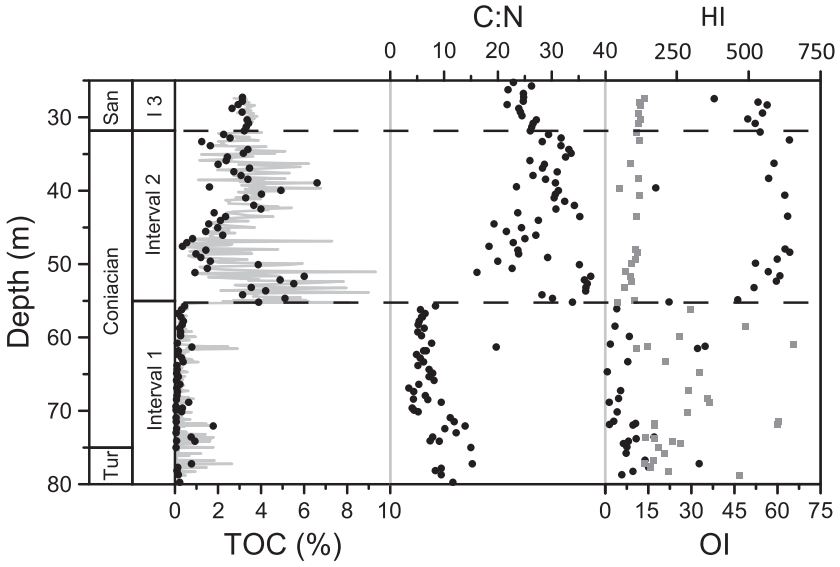

Figure 5. Total organic carbon (TOC), organic carbon to nitrogen (C:N) ratios, and Rock-Eval (H-Index and O-Index) results from the Portland core. Dashed lines indicate correlated intervals.

4.5. C:N and Rock-Eval

C:N ratios are plotted in Figure 5; Redfield ratio values are included as dashed lines for comparison. The C:N record generally covaries with TOC, with high ratios corresponding to elevated organic carbon samples. C:N values from Interval 1 average 8.4, which is within the range expected for marine phytoplankton derived organic matter [*Emerson and Hedges*, 1988]. However, the first half of Interval 1 records larger C:N values (mean = 10.3), as compared to the second half of Interval 1 (mean = 6.5). During Intervals 2 and 3, C:N ratios average 26.6, significantly above Redfield ratio values. Rock-Eval results from *Locklair* [2007] are also plotted in Figure 5. The H-index record exhibits trends similar to the C:N record, while the O-index record behaves opposite to the other organic proxies discussed here.

5. Discussion

5.1. Carbon Isotope Stratigraphy in the Late Cretaceous

Despite the lack of global organic carbon burial, a correlative broad positive $\delta^{13}C_{carb}$ excursion associated with OAE 3 has been identified in many localities, including those that do not exhibit black shale deposition [*Jenkyns et al.*, 1994; *De Romero et al.*, 2003]. A previously published record from the Berthoud State core demonstrates that WIS $\delta^{13}C_{carb}$ trends can be generally correlated to records globally [*Pratt et al.*, 1993; *Wendler*, 2013]. The Berthoud record, however, is highly variable and must be smoothed before attempting correlation [*Pratt et al.*, 1993; *Locklair et al.*, 2011; *Wendler*, 2013]. A new record presented herein from the USGS Portland core illustrates similar broad-scale trends to the Berthoud record, but provides a much less variable record for correlation, requiring less data manipulation to produce correlatable trends. The Portland record exhibits a clear two-step $\delta^{13}C_{carb}$ excursion from the base of the Fort Hays into the high organic carbon burial interval. The first step is a positive 1‰ shift, which corresponds to the onset of the Niobrara transgression (Figure 2). After an isotopic plateau, the $\delta^{13}C_{carb}$ record indicates a second positive 1‰ isotopic shift in the early Coniacian (Figure 2). This isotopic shift is coeval with the onset of regional enhanced burial of ^{13}C-depleted organic carbon and corresponds to the identified OAE 3 plateau in global and regional records (Figure S1 in the supporting information).

High-resolution $\delta^{13}C_{org}$ isotope records from the Niobrara interval of the Portland core lack a positive isotope excursion or plateau associated with the "OAE 3" interval [*Joo and Sageman*, 2014]. To address the inconsistency in the two reconstructions, paired $\delta^{13}C_{org}$ and $\delta^{13}C_{carb}$ data measured on the same samples are presented here (Figure 2). Our new $\delta^{13}C_{org}$ results similarly do not exhibit the OAE 3 isotope plateau and instead show generally more positive values as compared to other records from the WIS [*Joo and Sageman*, 2014]. The $\delta^{13}C_{org}$ results from the Portland core thus do not track $\delta^{13}C_{carb}$ records from the same core, or from other localities in the seaway, implying that secular changes in the marine carbon reservoir are overprinted by a local signal in the Portland $\delta^{13}C_{org}$ record. This is not the case for all $\delta^{13}C_{org}$ records within the WIS, as the record from the Aristocrat Angus Core exhibits a clearly identifiable OAE 3 excursion [*Joo and Sageman*, 2014]. The discrepancy in the Portland $\delta^{13}C_{org}$ record is discussed further below.

5.2. Redox History

The Portland geochemical records indicate that Fort Hays sediments were deposited under the most oxic conditions (Figure 4). Low Re and Mo concentrations high Mn concentrations, and high Re/Mo ratios indicate that the bottom waters in the WIS were well oxygenated and that the sediments were suboxic. Isolated clay-rich interbeds within the Fort Hays contain higher concentrations of organic carbon and trace metals than the more carbonate-rich facies, consistent with brief instances of increased carbon burial and oxygen limitation. However, significant bioturbation of the limestone beds suggests moderately to well-oxygenated substrates predominated during Interval 1 [*Savdra*, 1998].

During the second half of Interval 1, excess Mn concentrations and Re/Mo ratios increase, indicative of expanding suboxic conditions. However, the second half of Interval 1 remained largely bioturbated, but with burrow types and sizes indicating lower levels of oxygenation than within the Fort Hays [*Savdra*, 1998]. Notably, this gradual change in evidence for oxygen limitation is not paralleled by an increase in organic carbon or trace metal concentrations. It is not until a threshold or "tipping point" is reached that TOC and trace metal concentrations increase abruptly, at the onset of Interval 2 (OAE 3). The possibility of small hiatuses in the record near the transition from Intervals 1 to 2 exists that may have produced the

apparent abrupt tipping point or threshold. However, even if the transition into suboxic conditions was more gradual, the overall observation does not change that a threshold oxygen concentration was reached causing a distinct increase in TOC and trace metal accumulations.

High excess trace metal concentrations (Mo and Re), low Re/Mo ratios, and Mn concentrations below background levels indicate that reducing conditions prevailed in the WIS during both organic carbon burial peaks within Interval 2 (Figure 4). Mo concentrations (30–105 ppm) indicate that periods of intermittent to persistent euxinia likely occurred during the peak carbon burial [*Scott and Lyons*, 2012]. The absence of trace fossils and the presence of laminated strata during this period indicate that low bottom water oxygen concentrations prevented macrofauna from bioturbating sediments [*Savdra*, 1998].

Variations in trace metal accumulation and TOC during Interval 2 suggest that there were brief periods of increased oxygenation and reduced organic carbon burial during Interval 2 (Figure 5). The significantly reduced trace metal accumulation, paired with indistinct laminations, which are suggestive of some bioturbation, supports the conclusion that the middle of Interval 2 was associated with occasional oxygenation events of the bottom waters [*Savdra*, 1998]. However, even within this period, TOC concentrations remain significantly above those recorded during Interval 1 (<2%), suggesting that conditions did not return to those experienced prior to OAE 3. At the onset of Interval 3, trace metals and TOC shift to values between those found in Intervals 1 and 2. Although a change in bottom water oxygenation and/or marine productivity may have occurred from Intervals 2 to 3, marine environmental conditions did not return to those of Interval 1.

5.3. Redox-Controlled Degradation of Organic Matter

The effect of oxygen availability on organic matter (OM) preservation has been a longstanding focus of black shale studies [e.g., *Hunt*, 1996; *Demaison and Moore*, 1980; *Pedersen and Calvert*, 1990]; however, the exact relationship between water column anoxia and OM preservation remains a subject of active study [e.g., *Henrichs and Reeburgh*, 1987; *Arndt et al.*, 2013]. Complications include reactivity of OM, macrofaunal processes, oxygen exposure time, and redox oscillations [e.g., *Aller*, 1994; *Canfield*, 1994; *Arndt et al.*, 2013]. Organic matter preservation of TOC-rich sediments deposited in the WIS during OAE 2 has been studied by focusing on the relationship between Rock-Eval and bioturbation [*Pratt*, 1984], the role of sulfide formation and highly reactive iron availability [*Meyers et al.*, 2005], and the characteristics of individual organic molecules [*Hayes et al.*, 1989, 1990; *Pancost et al.*, 1998]. New results herein allow for the characterization of relationships between redox conditions, bioturbation, and the amount and composition of OM preserved during the prolonged organic carbon burial event recorded in the Niobrara Formation.

Observed variations in OM elemental composition (H- and O-Indices and C:N ratios) in the Portland core most likely record variations in the mode of OM remineralization under different redox conditions (Figures 6a and 6b).Variations in the elemental composition of OM can also indicate changes in OM source (i.e., dominantly terrestrial versus marine material) [*Meyers*, 1994; *Purdue and Koprivnjak*, 2007]. However, comparison of Rock-Eval and C:N ratios within the Portland core is difficult to interpret in terms of variable influences of terrestrial OM (Figure 6a). For example, the high C:N ratios (up to 40) measured during Interval 2 deviate from typical marine OM and could be consistent with the signature of C3 plant OM [*Meyers*, 2006], but H- and O-Index values indicate a predominantly marine origin.

C:N values in the Portland core covary with redox conditions reconstructed from trace metal records (Figure 6). Under the well-oxygenated conditions characteristic of deposition during Interval 1, C:N values are consistent with typical marine OM, which has C:N values of 5–8 [*Emerson and Hedges*, 1988; *Meyers*, 2006]. Elevated C:N values recorded during the first half of Interval 1 are associated with slightly elevated TOC and H-index values and may be indicative of brief periods of minor oxygen limitation in the shale interbeds of the FHL. Upon development of water column anoxia, C:N ratios increase sharply to between 15 and 40, similar to elevated C:N ratios of marine OM found in sapropels, Cretaceous black shales, and recent sediments deposited under upwelling regions [*Meyers*, 2006; *Junium and Arthur*, 2007]. Incubation experiments and modern observations suggest that a suboxic water column affects the composition of residual organic material as well as the rate of OM degradation, supporting preferential degradation of N-rich proteins and preservation of N-poor lipids [*Harvey et al.*, 1995; *Van Mooy et al.*, 2002]. Proteins and carbohydrates are more susceptible to degradation because they contain N and O functional groups, while lipids contain more hydrocarbon-like carbon chains that make them less degradable [*Meyers*, 2014].

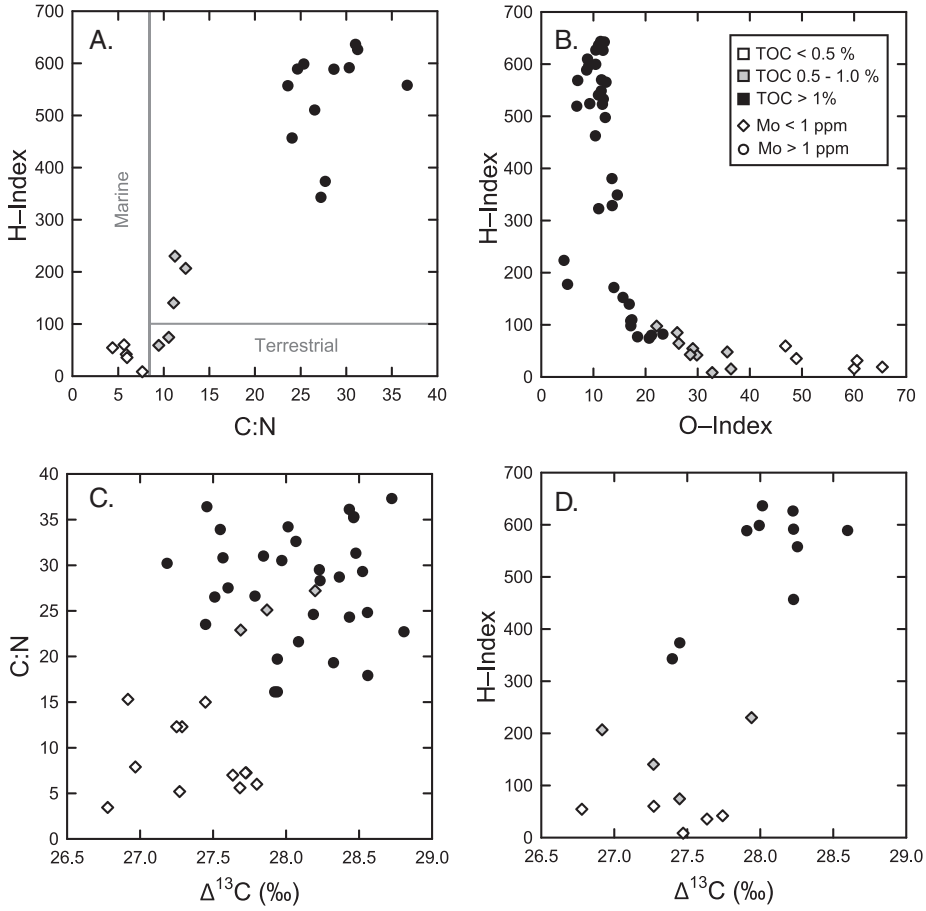

Figure 6. (a) C:N and H-Index crossplot with typical terrestrial and marine organic matter labeled, (b) H-Index and O-Index crossplot, (c) C:N and $\Delta^{13}C$ crossplot, and (d) H-Index and $\Delta^{13}C$ crossplot. Mo concentrations are plotted as diamonds (<1 ppm) or circles (>1 ppm). TOC concentrations are plotted as white (<0.5%), gray (0.5–1.0%), or black (>1.0%).

Furthermore, anaerobic bacteria are less able to depolymerize certain large complex molecules including saturated hydrocarbons and lignin than aerobic bacteria [*Benner et al.*, 1984; *Schink*, 1988; *Kristensen*, 2000]. Model results indicate that complete removal of N-rich amino acids and nucleic acids can increase the C:N ratio, but that the accumulation of marine OM with C:N ratios of >20 during the Late Cretaceous requires an additional mechanism, such as ammonium loss under euxinic conditions [*Junium and Arthur*, 2007].

Rock-Eval results support a shift toward preferential preservation of lipids as O-poor, H-rich organic matter characterizes Intervals 2 and 3. Similar to results from the Greenhorn Formation [*Pratt*, 1984], our data from the Niobrara Formation indicate that changes in H- and O-Indices are closely linked to changes in bioturbation. Bioturbation influences the composition of the pore water and solid constituents in sediments when infaunal animals ventilate the substrate with oxygen-rich waters, stimulating microbial activity [*Aller*, 1978; *Kristensen*, 2000; *Zonneveld et al.*, 2010]. When oxygen limitation reduces macrofaunal activity, the loss of these processes provides a positive feedback to the development of anoxia. In moderately to highly bioturbated sections, burrowing organisms and the associated oxidative processes result in near complete OM loss from the sediments, while poorly oxygenated conditions preserve significant hydrogen-rich OM in laminated or microbioturbated sediments.

Comparison of C:N and Rock-Eval results with the TOC record supports a direct effect of changing redox conditions on the amount of TOC preserved within sediments (Figure 6). Interval 1 is characterized by dominantly aerobic degradation of OM facilitated by significant bioturbation that removes almost all OM from the sediments. A shift occurs at the beginning of Interval 2 to anaerobic degradation of OM that coincides with the distinct increase in the amount of TOC preserved within sediments. This suggests that a

shift in the mode of OM recycling acts as the trigger of black shale (>1% TOC) deposition within the Portland core, whereby OM preservation increased once a threshold redox condition was met.

5.4. Variations in $\Delta^{13}C$

In addition to variations in the elemental composition of organic matter, $\Delta^{13}C$ values highlight that changes in OM degradation can alter primary $\delta^{13}C_{org}$ signals (Figure 2). Calculation of $\Delta^{13}C$ is one approach for evaluating changes in the relationship between the isotopic records of carbonate, representing the dissolved inorganic carbon pool, and OM, representing the photosynthate pool. Several factors can influence the carbon isotope fractionation factor itself (ε_p), such as changes in pCO_2 or the growth rate of photosynthesizers (controlled by nutrient availability), and the preserved isotopic records may be subject to postdepositional alteration, including carbonate diagenesis affecting the $\delta^{13}C_{carb}$ record or OM degradation influencing the $\delta^{13}C_{org}$ record; in addition, variations in the contributions of OM from different sources can also influence the $\delta^{13}C_{org}$ signal (*Popp et al.*, 1989; *Freeman and Hayes*, 1992; *Kump and Arthur*, 1999; *Kienast et al.*, 2001; *Royer et al.*, 2001; *Pagani et al.*, 2002). As such, attempts to employ $\Delta^{13}C$ as a proxy for changes in pCO_2 [e.g., *Jarvis et al.*, 2011] require that all other potential influences be ruled out.

Although the $\delta^{13}C_{carb}$ values used in our calculation are bulk data rather than pristine shell carbonate, they are derived from chalky lithologies that are dominated by nannofossil shell material. In addition, the lack of diagenetic covariation between $\delta^{13}C_{carb}$ versus $\delta^{18}O_{carb}$ and the presence of the OAE 3 $\delta^{13}C_{carb}$ plateau that is found in global and regional $\delta^{13}C$ records suggests that diagenesis has not significantly altered our $\delta^{13}C_{carb}$ record (Figures S1 and S2). There are several indications, however, that the OM record does not preserve the isotopic signature of primary photosynthate.

For example, coeval shifts in C:N ratios, H-indices, and $\Delta^{13}C$ values in the Portland core suggest that changes in redox-controlled OM degradation affected both the isotopic and elemental composition of the preserved sedimentary OM (Figure 6). On one hand, the oxidative degradation of OM in Interval 1 may have led to preferential preservation of material with a more positive $\delta^{13}C_{org}$ signature. On the other hand, preservation of H-rich OM in laminated black shale facies can produce anomalous $\delta^{13}C_{org}$ values that would influence the $\Delta^{13}C$ calculation [*Joachimski*, 1997]. For example, marine lipids are depleted in $\delta^{13}C_{org}$ by 8–10‰ relative to marine carbohydrates and proteins [*Degens et al.*, 1968], and the effect of selective diagenesis can alter $\delta^{13}C_{org}$ by 2–3‰ [*Dean et al.*, 1986; *Meyers*, 2014]. Thus, the preferential preservation of H-rich OM in Interval 2 may have led to $\delta^{13}C_{org}$ values that are depleted relative to primary values. These results indicate that redox-controlled isotope effects should be considered before $\delta^{13}C_{org}$ records are used for stratigraphy or pCO_2 reconstructions.

5.5. Mechanisms for the Development of Anoxia

New results indicate that changes in redox conditions were of primary importance in the amount of OM preserved and its elemental and isotopic composition. Sediment pore water and bottom water oxygenation distinctly changed between the three intervals highlighted in the Portland core, but multiple causes for the development of low-oxygen conditions are possible. Previous work within the WIS has highlighted the importance of reduced ventilation of bottom waters [*Pratt*, 1984; *Barron et al.*, 1985; *Kauffman*, 1988; *Hay et al.*, 1993], increased oxidant demand associated with elevated export productivity [*Watkins*, 1989], or a combination of the two with highly productive surface waters overlying seasonally or intermittently stratified bottom waters [*Tyson and Pearson*, 1991; *Sageman and Bina*, 1997; *Arthur and Sageman*, 2005; *Meyers et al.*, 2005; *White and Arthur*, 2006].

5.5.1. Stratification

Stable or seasonal stratification has been invoked as a mechanism for the development of anoxia within the WIS by many authors [e.g., *Pratt*, 1984; *Sageman*, 1989; *Arthur and Sageman*, 2005]. Variations in sea level within the shallow WIS may have aided in the development of stratification as a deeper water column would reduce the influence of wind driven and tidal mixing. The role of sea level on the development of stable salinity stratification has been discussed for the WIS in association with the deposition of organic carbon-rich sediments of the Greenhorn Formation. This interpretation is based on the relationship between changes in current-induced sedimentary structures, extent of bioturbation, and organic carbon accumulation [*Pratt*, 1984]. The Niobrara Formation was deposited during the Niobrara second order

marine cycle [*Kauffman*, 1977], which is comparable to the Greenhorn marine cycle in terms of interpreted sea level rise and flooding extent [*Kauffman and Caldwell*, 1993]. Paleontological and sedimentary evidence indicate that the Fort Hays was initially deposited in water depths of 15–50 m and that the water column progressively deepened to water depths of 150–300 m during Smoky Hill deposition [*Hattin*, 1982].

Prolonged stratification within the WIS would require a significant density contrast between surface and bottom waters. New $\delta^{18}O$ results suggest that despite significant variability within the Fort Hays shale-limestone couplets, deposition during Interval 1 was generally characterized by more normal marine salinity, and deposition during Intervals 2 and 3 was characterized by comparatively reduced salinity perhaps consistent with development of a low-salinity surface layer (Figure 3). Although new $\delta^{18}O$ results were measured on bulk carbonates, which can be susceptible to diagenetic alteration, $\delta^{18}O$ values and patterns are similar to inoceramid $\delta^{18}O$ results from nearby Lyons, Colorado, which indicate a shift from normal marine to more brackish conditions within the lower Smoky Hill [*Pratt and Barlow*, 1985]. A significant freshwater contribution to water masses is supported by fossil- and biophosphate-derived oxygen isotope evidence from throughout the WIS, as well as low diversity of surface dwelling organisms [*Tourtelot and Rye*, 1969; *Hattin*, 1982; *Wright*, 1987; *Fisher and Arthur*, 2002; *Coulson et al.*, 2011]. Continental paleoprecipitation estimates suggest that the increased freshwater influence may be derived from elevated runoff from the Sevier Highlands [*Retallack*, 2009], while shifts to more Boreal faunal communities support dominance of fresher, northern sourced surface water [*Da Gama et al.*, 2014]. Although the freshwater influence would aid in development of stratification, previous studies from the WIS suggest that ventilation events occurred even within TOC-rich units [*Sageman*, 1989; *Sageman and Bina*, 1997], which is consistent with variability in TOC and redox indicators in the Niobrara, specifically from 45 to 51 m in the Portland core. However, these variations might also be caused by reduced export productivity or changes in bottom water source area and/or ventilation.

Mo/TOC ratios within the Portland core further support the development of significant bottom water restriction, as would be expected with a water column subject to frequent and/or prolonged stratification. Mo/TOC ratios have been used as a proxy for the degree of restriction in ancient silled basins based on measurements from modern silled basins including the Black Sea, Cariaco Basin, Framvaren Fjord, and Saanich Inlet [*Algeo and Lyons*, 2006]. The average Mo/TOC ($\times 10^{-4}$) for Intervals 2 and 3 within the Portland core is 5.6 (with a range of 1.2 to 17.4). These values are most similar to those of the Framvaren Fjord (4.5 ± 1) and the Black Sea (9 ± 2), the most restricted of the modern anoxic basins studied, suggesting that the WIS experienced significant bottom water restriction throughout the period of enhanced carbon burial.

Taken together, the observations cited above suggest that stratification played an important role in Western Interior carbon burial during the Coniacian-Santonian. The Fort Hays Limestone was deposited in a shallow well-mixed and well-oxygenated water column, and under these conditions, OM was nearly completely oxidized. As the water column progressively deepened and the freshwater influence increased, significant water column stratification developed, leading to a prolonged dominance of oxygen deficiency within bottom waters. When conditions became sufficiently oxygen limited, changes in OM remineralization fueled elevated TOC accumulation within sediments.

5.5.2. Nutrient Input and Recycling

Studies of the Cenomanian-Turonian have argued that elevated productivity is of primary importance for the development of OAEs. Enhanced organic carbon burial in the late Cenomanian was likely initiated due to increased nutrient input from both volcanogenic and continental sources [*Adams et al.*, 2010; *Du Vivier et al.*, 2014]. Extreme trace metal enrichment [*Brumsack*, 2006; *Snow et al.*, 2005], interpreted to reflect significant increases in volcanogenically sourced nutrients during OAE2, does not exist for the Coniacian-Santonian. However, continental runoff may have influenced nutrient availability within the seaway, as nannofossil and palynology studies from the Niobrara Formation show a relationship between increased freshwater runoff and surface water fertility [*Burns and Bralower*, 1998; *Da Gama et al.*, 2014].

Lithogenic element concentrations, such as Al, might be expected to increase with an increased flux of detrital material and nutrients to the seaway. However, interpreting Al concentrations is difficult because they are controlled by both the amount of detrital input and carbonate dilution. The relationship between Al and TOC concentrations is unclear as Al concentrations fluctuate throughout the record with no distinct

change associated with the onset of organic carbon burial (Figure 3). Therefore, better constraints on sediment provenance, terrestrial weathering, and hydrology are required to confirm a relationship between carbon burial and terrestrially derived nutrient input into the WIS.

Changes in benthic regeneration of nutrients could also play a significant role in sustaining primary productivity. Cretaceous ocean modeling studies suggest that enhanced P regeneration from anoxic sediments facilitated black shale deposition during OAE 2 [*Handoh and Lenton*, 2003; *Nederbragt et al.*, 2004; *Bjerrum et al.*, 2006; *Tsandev and Slomp*, 2009], while evidence of enhanced P recycling during OAE 2 has been found from the Tethys, WIS, and proto-Atlantic Ocean [*Mort et al.*, 2007; *Tsandev and Slomp*, 2009; *Kraal et al.*, 2010]. Better constraints are required to assess changes in nutrient recycling within the seaway, but enhanced productivity and an increased oxidant demand could have exacerbated the oxygen limitation and the accumulation of TOC within the WIS.

6. Conclusions

The $\delta^{13}C_{carb}$ record from the Portland core illustrates that the bulk carbonate carbon isotope record is correlatable between regional and global records in the seaway during the Late Cretaceous. The trends within the Portland core indicate a two-step positive $\delta^{13}C_{carb}$ excursion during the Late Turonian and early Coniacian that corresponds to (1) the Niobrara sea level transgression and (2) regional carbon burial that has been previously identified as OAE 3. Calculated $\Delta^{13}C$ values indicate a decoupling between $\delta^{13}C_{carb}$ and $\delta^{13}C_{org}$ during this time.

Significant quantities of organic carbon are preserved in the Niobrara Formation, demonstrating that the WIS sustained extended periods of organic carbon burial during the Coniacian-Santonian. Records of redox sensitive metals indicate deposition within a well-oxygenated, shallow seaway during initial transgression that became increasingly oxygen limited as the water column deepened, with the onset of significant oxygen depletion preceding the onset of organic carbon burial. The abrupt shift in TOC accumulation was associated with a redox-controlled shift in OM alteration. Coupled C:N, H-Index, O-Index, and Mo results indicate a shift from dominantly aerobic degradation of OM during Interval 1 to more anaerobic degradation during Intervals 2 and 3. $\Delta^{13}C$ values covary with changes in the elemental composition of OM suggesting a redox control on the decoupling of $\delta^{13}C_{carb}$ and $\delta^{13}C_{org}$ during this time, suggesting that variable redox conditions can complicate the use of $\delta^{13}C_{org}$ for stratigraphy of pCO_2 reconstructions. The correspondence between TOC, redox sensitive metals, and organic proxies indicates that the redox shift caused an increase in the amount of TOC preserved in the sediments. Sea level reconstructions, $\delta^{18}O$ results, and Mo/TOC ratios suggest that stratification and bottom water restriction caused the drawdown of bottom water oxygen. Increased nutrients from benthic regeneration, open ocean import, and/or runoff from the Sevier Highlands may have helped sustain primary productivity, providing a significant oxidant demand throughout the prolonged period of organic carbon burial.

Acknowledgments

Data presented in this paper will be available on the Pangea website (http://www.pangaea.de). We are grateful to Phil Meyers for thoughtful discussions and manuscript comments. We would like to thank Lora Wingate for help with stable isotope analyses. We would also like to thank Danielle Boshers for sample processing. We are grateful to the USGS Core Research Center for sample collection. This work was supported by ACS-PRF grant (#53845-ND8) to N.D.S. and I.H. and a Scott Turner Award from the Department of Earth and Environmental Sciences at UM. A.T. was supported by an NSF-GRF (DGE 1256260).

References

Adams, D. D., M. T. Hurtgen, and B. B. Sageman (2010), Volcanic triggering of a biogeochemical cascade during Oceanic Anoxic Event 2, *Nat. Geosci.*, *3*(3), 201–204.

Algeo, T. J., and T. W. Lyons (2006), Mo–total organic carbon covariation in modern anoxic marine environments: Implications for analysis of paleoredox and paleohydrographic conditions, *Paleoceanography*, *21*, PA1016, doi:10.1029/2004PA001112.

Aller, R. C. (1978), Experimental studies of changes produced by deposit feeders on pore water, sediment and overlying water chemistry, *Am. J. Sci.*, *278*, 1185–1234.

Aller, R. C. (1994), Bioturbation and remineralization of sedimentary organic matter: Effects of redox oscillation, *Chem. Geol.*, *3–4*, 331–345.

Arndt, S., B. B. Jørgensen, D. E. LaRowe, J. J. Middelburg, R. D. Pancost, and P. Regnier (2013), Quantifying the degradation of organic matter in marine sediments: A review and synthesis, *Earth Sci. Rev.*, *123*, 53–86.

Arthur, M. A., and B. B. Sageman (1994), Marine black shales: Depositional mechanisms and environments of ancient deposits, *Annu. Rev. Earth Planet. Sci.*, *22*, 499–551.

Arthur, M. A., and B. B. Sageman (2005), Sea level control on source rock development: Perspectives from the Holocene Black Sea, the mid-Cretaceous Western Interior Basin of North America, and the Late Devonian Appalachian Basin, in *Deposition of Organic-Carbon-Rich Sediments: Models, Mechanisms, and Consequences*, edited by N. B. Harris, pp. 35–59, SEPM, Tulsa, Okla.

Arthur, M. A., S. O. Schlanger, and H. C. Jenkyns (1987), The Cenomanian-Turonian Oceanic Anoxic Event, II. Paleoceanographic controls on organic matter production and preservation, in *Marine Petroleum Source Rocks, Geological Society of London Special Paper*, edited by J. A. A. F. Brooks, pp. 401–420, Blackwell, Oxford, U. K.

Barron, E. J., M. A. Arthur, and E. G. Kauffman (1985), Cretaceous rhythmic bedding sequences: A plausible link between orbital variations and climate, *Earth Planet. Sci. Lett.*, *72*(4), 327–340.

Beckmann, B., T. Wagner, and P. Hofmann (2005), Linking Coniacian-Santonian (OAE 3) black shale deposition to African climate variability: A reference section from the eastern tropical Atlantic at orbital time scales (ODP 959, off Ivory Coast and Ghana), in *Deposition of Organic-Carbon-Rich Sediments: Models, Mechanisms, and Consequences*, edited by N. B. Harris, pp. 125–143, SEPM, Tulsa, Okla.

Benner, R., A. E. Maccubbin, and R. E. Hodson (1984), Anaerobic biodegradation of the lignin and polysaccharide components of lignocellulose and synthetic lignin by sediment microflora, *Appl. Environ. Microbiol.*, *47*, 998–1004.

Bjerrum, C. J., J. Bendtsem, and J. J. F. Legarth (2006), Modeling organic carbon burial during sea level rise with reference to the Cretaceous, *Geochem. Geophys. Geosyst.*, *7*, Q05008, doi:10.1029/2005GC001032.

Bohacs, K. M., G. J. Grabowski Jr., A. R. Carroll, P. J. Mankiewicz, K. J. Miskell-Gerhardt, J. R. Schwalbach, M. B. Wegner, and J. A. Simo (2005), Production, destruction, and dilution—The many paths to source-rock development, in *The Deposition of Organic-Carbon-Rich Sediments: Models, Mechanisms, and Consequences, SEPM Spec. Publ.*, vol. 82, edited by N. Harris, pp. 61–101, SEPM, Tulsa, Okla.

Brumsack, H. J. (2006), The trace metal content of recent organic carbon-rich sediments: Implications for Cretaceous black shale formation, *Palaeogeogr. Palaeoclimatol. Palaeoecol.*, *232*(2–4), 344–361.

Burns, C. E., and T. J. Bralower (1998), Upper Cretaceous nannofossil assemblages across the Western Interior Seaway: Implications for the origins of lithologic cycles in the Greenhorn and Niobrara Formations, in *Stratigraphy and Paleoenvironments of the Cretaceous Western Interior Seaway*, edited by W. E. Dean and M. A. Arthur, pp. 227–255, SEPM Concepts in Sedimentology and Paleontology, Tulsa, Okla.

Calvert, S. E., and T. F. Pedersen (1993), Geochemistry of recent oxic and anoxic marine sediments—Implications for the geologic record, *Mar. Geol.*, *113*(1–2), 67–88.

Canfield, D. E. (1994), Factors influencing organic carbon preservation in marine sediments, *Chem. Geol.*, *114*, 315–329.

Coulson, A. B., M. J. Kohn, and R. E. Barrick (2011), Isotopic evaluation of ocean circulation in the Late Cretaceous North American seaway, *Nat. Geosci.*, *4*(12), 852–855.

Crusius, J., S. Calvert, T. Pedersen, and D. Sage (1996), Rhenium and molybdenum enrichments in sediments as indicators of oxic, suboxic and sulfidic conditions of deposition, *Earth Planet. Sci. Lett.*, *145*(1–4), 65–78.

Da Gama, R. O. B. P., B. Lutz, P. Desjardins, M. Thompson, I. Prince, and I. Espejo (2014), Integrated paleoenvironmental analysis of the Niobrara Formation: Cretaceous Western Interior Seaway, northern Colorado, *Palaeogeogr. Palaeoclimatol. Palaeoecol.*, *413*, 66–80.

De Romero, L. M., I. M. Truskowski, T. J. Bralower, J. A. Bergen, O. Odreman, J. C. Zachos, and F. A. Galea-Alvarez (2003), An integrated calcareous microfossil biostratigraphic and carbon-isotope stratigraphic framework for the La Luna Formation, western Venezuela, *Palaios*, *18*(4–5), 349–366.

Dean, W. E., and M. A. Arthur (1998), Geochemical expressions of cyclicity in Cretaceous pelagic limestone sequences: Niobrara Formation, Western Interior Seaway, in *Stratigraphy and Paleoenvironments of the Cretaceous Western Interior Seaway*, edited by W. E. Dean and M. A. Arthur, pp. 227–255, SEPM Concepts in Sedimentology and Paleontology, Tulsa, Okla.

Dean, W. E., M. A. Arthur, and G. E. Claypool (1986), Depletion of 13 C in Cretaceous marine organic matter: Source, diagenetic, or environmental signal?, *Mar. Geol.*, *70*(1), 119–157.

Degens, E. T., M. Behrendt, B. V. Gotthardt, and E. Reppmann (1968), Metabolic fractionation of carbon isotopes in marine plankton, *Deep Sea Res. Oceanogr. Abstr.*, *15*, 11–20.

Demaison, G. J., and G. T. Moore (1980), Anoxic environments and oil source bed genesis, *Am. Assoc. Pet. Geol. Bull.*, *64*, 1179–1209.

Du Vivier, A. D. C., D. Selby, B. B. Sageman, I. Jarvis, D. R. Groecke, and S. Voigt (2014), Marine Os-187/Os-188 isotope stratigraphy reveals the interaction of volcanism and ocean circulation during Oceanic Anoxic Event 2, *Earth Planet. Sci. Lett.*, *389*, 23–33.

Emerson, S., and J. I. Hedges (1988), Processes controlling the organic carbon content of open ocean sediments, *Paleoceanography*, *3*, 621–634, doi:10.1029/PA003i005p00621.

Espitalie, J., J. L. Laporte, M. Madec, F. Marquis, P. Leplat, J. Paulet, and A. Boutefeu (1977), Rapid method for source rock characterization, and for determination of their petroleum potential and degree of evolution, *Rev. Inst. Fr. Pet. Ann. Combust. Liq.*, *32*(1), 23–42.

Fisher, C. G., and M. A. Arthur (2002), Water mass characteristics in the Cenomanian US Western Interior seaway as indicated by stable isotopes of calcareous organisms, *Palaeogeogr. Palaeoclimatol. Palaeoecol.*, *188*(3–4), 189–213.

Fisher, C. G., W. W. Hay, and D. L. Eicher (1994), Oceanic front in the Greenhorn Sea (Late Middle through Late Cenomanian), *Paleoceanography*, *9*(6), 879–892, doi:10.1029/94PA02114.

Floegel, S., W. W. Hay, R. M. DeConto, and A. N. Balukhovsk (2005), Formation of sedimentary bedding couplets in the Western Interior Seaway of North America—Implications from climate system modeling, *Palaeogeogr. Palaeoclimatol. Palaeoecol.*, *218*(1–2), 125–143.

Freeman, K. H., and J. M. Hayes (1992), Fractionation of carbon isotopes by phytoplankton and estimates of ancient CO_2 levels, *Global Biogeochem. Cycles*, *6*(2), 185–198, doi:10.1029/92GB00190.

Handoh, I. C., and T. M. Lenton (2003), Periodic mid-Cretaceous oceanic anoxic events linked by oscillations of the phosphorus and oxygen biogeochemical cycles, *Global Biogeochem. Cycles*, *17*(4), 1092, doi:10.1029/2003GB002039.

Hartnett, H. E., R. G. Keil, J. I. Hedges, and A. H. Devol (1998), Influence of oxygen exposure time on organic carbon preservation in continental margin sediments, *Nature*, *391*, 572–575, doi:10.1038/35351.

Harvey, H. R., J. H. Tuttl, and J. T. Bell (1995), Kinetics of phytoplankton decay during simulated sedimentation: Changes in biochemical composition and microbial activity under oxic and anoxic conditions, *Geochim. Cosmochim. Acta*, *59*, 3367–3377.

Hattin, D. E. (1982), Stratigraphy and depositional environment of Smoky Hill Chalk Member, Niobrara Chalk (Upper Cretaceous) of the type area, Western Kansas, *Kansas Geol. Soc. Bull.*, *225*, 108.

Hay, W. W., D. L. Eicher, and R. Diner (1993), Physical oceanography and water masses in the Cretaceous Western Interior Seaway, in *Evolution of the Western Interior Basin, GAC Spec. Pap.*, edited by W. G. E. Caldwell and E. G. Kauffman, pp. 333–354, Geol. Assoc. of Canada, Toronto.

Hayes, J. M., B. N. Popp, R. Takigiku, and M. W. Johnson (1989), An isotopic study of biogeochemical relationships between carbonates and organic matter in the Greenhorn Formation, *Geochim. Cosmochim. Acta*, *53*, 2961–2972.

Hayes, J. M., K. H. Freeman, B. N. Popp, and C. H. Hoham (1990), Compound-specific isotopic analyses: A novel tool for reconstruction of ancient biogeochemical processes, *Org. Geochem.*, *16*(4), 1115–1128.

Helz, G. R., C. V. Miller, J. M. Charnock, J. F. W. Mosselmans, R. A. D. Pattrick, C. D. Garner, and D. J. Vaughan (1996), Mechanism of molybdenum removal from the sea and its concentration in black shales: EXAFS evidence, *Geochim. Cosmochim. Acta*, *60*(19), 3631–3642.

Henrichs, S. M., and W. S. Reeburgh (1987), Anaerobic mineralization of marine sediment organic matter: Rates and the role of anaerobic processes in the oceanic carbon economy, *Geomicrobiol. J.*, *5*, 191–237.

Hild, E., and H. J. Brumsack (1998), Major and minor element geochemistry of Lower Aptian sediments from the NW German Basin (core Hoheneggelsen KB 40), *Cretaceous Res.*, *19*(5), 615–633.

Hofmann, P., T. Wagner, and B. Beckmann (2003), Millennial- to centennial-scale record of African climate variability and organic carbon accumulation in the Coniacian-Santonian eastern tropical Atlantic (Ocean Drilling Program Site 959, off Ivory Coast and Ghana), *Geology*, *31*(2), 135–138.

Hunt, J. M. (1996), *Petroleum Geochemistry and Geology*, Freeman Press, New York.

Jarvis, I., A. S. Gale, H. C. Jenkyns, and M. A. Pearce (2006), Secular variation in Late Cretaceous carbon isotopes: A new delta C-13 carbonate reference curve for the Cenomanian-Campanian (99.6–70.6 Ma), *Geol. Mag.*, *143*(5), 561–608.

Jarvis, I., J. S. Lignum, D. R. Grocke, H. C. Jenkyns, and M. A. Pearce (2011), Black shale deposition, atmospheric CO_2 drawdown, and cooling during the Cenomanian-Turonian Oceanic Anoxic Event, *Paleoceanography*, *26*, PA3201, doi:10.1029/2010PA002081.

Jenkyns, H. C. (2010), Geochemistry of oceanic anoxic events, *Geochem. Geophys. Geosyst.*, *11*, Q03004, doi:10.1029/2009GC002788.

Jenkyns, H. C., A. S. Gale, and R. M. Corfield (1994), Carbon-isotope and oxygen isotope stratigraphy of the English Chalk and Italian Scaglia and its paleoclimatic significance, *Geol. Mag.*, *131*(1), 1–34.

Joachimski, M. M. (1997), Comparison of organic and inorganic carbon isotope patterns across the Frasnian–Famennian boundary, *Palaeogeogr. Palaeoclimatol. Palaeoecol.*, *132*(1), 133–145.

Joo, Y. J., and B. B. Sageman (2014), Cenomanian to Campanian carbon isotope chemostratigraphy from the Western Interior Basin, USA, *J. Sediment. Res.*, *84*(7), 529–542.

Junium, C. K., and M. A. Arthur (2007), Nitrogen cycling during the Cretaceous, Cenomanian-Turonian oceanic anoxic event II, *Geochem. Geophys. Geosyst.*, *8*, Q03002, doi:10.1029/2006GC001328.

Kauffman, E. G. (1977), Geological and biological overview: Western Interior Cretaceous Basin, in *Cretaceous Facies, Faunas and Paleoenvironments Across the Western Interior Basin*, edited by E. G. Kauffman, pp. 75–99, Mountain Geologist, Denver, Colo.

Kauffman, E. G. (1988), Concepts and methods of high-resolution event stratigraphy, *Annu. Rev. Earth Planet. Sci.*, *16*, 605–654.

Kauffman, E. G., and W. G. E. Caldwell (1993), The Western Interior basin in space and time, in *Evolution of the Western Interior Basin*, edited by W. G. E. Caldwell and E. G. Kauffman, pp. 1–30, Geol. Assoc. of Canada, Toronto, Ontario.

Kennedy, M. J., and T. Wagner (2011), Clay mineral continental amplifier for marine carbon sequestration in a greenhouse ocean, *Proc. Natl. Acad. Sci.*, *108*, 9776–9781.

Kennedy, M. J., D. Pevear, and R. Hill (2002), Mineral surface control of organic carbon in black shale, *Science*, *295*, 657–660.

Kienast, M., S. E. Calvert, C. Pelejero, and J. O. Grimalt (2001), A critical review of marine sedimentary δ^{13}Corg-pCO2 estimates: New palaeorecords from the South China Sea and a revisit of other low-latitude δ^{13}Corg-pCO2 records, *Global Biogeochem. Cycles*, *15*(1), 113–127, doi:10.1029/2000GB001285.

Kraal, P., C. P. Slomp, A. Forster, and M. M. M. Kuypers (2010), Phosphorus cycling from the margin to abyssal depths in the proto-Atlantic during oceanic anoxic event 2, *Palaeogeogr. Palaeoclimatol. Palaeoecol.*, *295*(1), 42–54.

Kristensen, E. (2000), Organic matter diagenesis at the oxic/anoxic interface in coastal marine sediments, with emphasis on the role of burrowing animals, *Hydrobiologia*, *426*, 1–24.

Kump, L. R., and M. A. Arthur (1999), Interpreting carbon-isotope excursions: Carbonates and organic matter, *Chem. Geol.*, *161*(1), 181–198.

Locklair, R. E. (2007), Causes and consequences of marine carbon burial: Examples from the Cretaceous Niobrara Formation and the Permian Brushy Canyon Formation, unpublished PhD thesis, Northwestern Univ., p. 515.

Locklair, R. E., and B. B. Sageman (2008), Cyclostratigraphy of the Upper Cretaceous Niobrara Formation, Western Interior, USA: A Coniacian-Santonian orbital timescale, *Earth Planet. Sci. Lett.*, *269*(3–4), 539–552.

Locklair, R., B. Sageman, and A. Lerman (2011), Marine carbon burial flux and the carbon isotope record of Late Cretaceous (Coniacian-Santonian) Oceanic Anoxic Event III, *Sediment. Geol.*, *235*(1–2), 38–49.

Marz, C., S. W. Poulton, B. Beckmann, K. Kuester, T. Wagner, and S. Kasten (2008), Redox sensitivity of P cycling during marine black shale formation: Dynamics of sulfidic and anoxic, non-sulfidic bottom waters, *Geochim. Cosmochim. Acta*, *72*(15), 3703–3717.

McLennan, S. M. (2001), Relationships between the trace element composition of sedimentary rocks and upper continental crust, *Geochem. Geophys. Geosyst.*, *2*, 1021, doi:10.1029/2000GC000109.

Meyers, P. A. (1994), Preservation of elemental and isotopic source identification of sedimentary organic matter, *Chem. Geol.*, *114*(3), 289–302.

Meyers, P. A. (2006), Paleoceanographic and paleoclimatic similarities between Mediterranean sapropels and Cretaceous black shales, *Palaeogeogr. Palaeoclimatol. Palaeoecol.*, *235*(1–3), 305–320.

Meyers, P. A. (2014), Why are the δ^{13}Corg values in Phanerozoic black shales more negative than in modern marine organic matter?, *Geochem. Geophys. Geosyst.*, *15*, 3085–3106, doi:10.1002/2014GC005305.

Meyers, S. R., and B. B. Sageman (2004), Detection, quantification, and significance of hiatuses in pelagic and hemipelagic strata, *Earth Planet. Sci. Lett.*, *224*, 55–72.

Meyers, S. R., B. B. Sageman, and T. W. Lyons (2005), Organic carbon burial rate and the molybdenum proxy: Theoretical framework and application to Cenomanian-Turonian oceanic anoxic event 2, *Paleoceanography*, *20*, PA2002, doi:10.1029/2004PA001068.

Morford, J. L., A. D. Russell, and S. Emerson (2001), Trace metal evidence for changes in the redox environment associated with the transition from terrigenous clay to diatomaceous sediment, Saanich Inlet, BC, *Mar. Geol.*, *174*(1–4), 355–369.

Mort, H. P., T. Adatte, K. B. Follmi, G. Keller, P. Steinmann, V. Matera, Z. Berner, and D. Stuben (2007), Phosphorus and the roles of productivity and nutrient recycling during oceanic anoxic event 2, *Geology*, *35*, 483–486.

Muller-Karger, F. E., R. Varela, R. Thunell, R. Luerssen, C. M. Hu, and J. J. Walsh (2005), The importance of continental margins in the global carbon cycle, *Geophys. Res. Lett.*, *32*, L01602, doi:10.1029/2004GL021346.

Nederbragt, A. J., J. W. Thurow, H. Vonhof, and H.-J. Brumsack (2004), Modelling oceanic carbon and phosphorus fluxes: Implications for the cause of the late Cenomanian Oceanic Anoxic Event (OAE2), *J. Geol. Soc.*, *161*(4), 721–728.

Pagani, M., K. H. Freeman, K. Ohkouchi, and K. Caldeira (2002), Comparison of water column [CO_{2aq}] with sedimentary alkenone-based estimates: A test of the alkenone-CO_2 proxy, *Paleoceanography*, *17*(4), 1069, doi:10.1029/2002PA000756.

Pancost, R. D., K. A. Freeman, and M. A. Arthur (1998), Arthur Organic geochemistry of the Cretaceous Western Interior Seaway: A trans-basinal evaluation, in *Stratigraphy and Paleoenvironments of the Cretaceous Western Interior Seaway*, edited by W. E. Dean and M. A. Arthur, pp. 227–255, SEPM Concepts in Sedimentology and Paleontology, Tulsa, Okla.

Pedersen, T. F., and S. E. Calvert (1990), Anoxia vs. productivity: What controls the formation of organic-carbon-rich sediments and sedimentary rocks?, *Am. Assoc. Pet. Geol. Bull.*, *74*, 454–466.

Popp, B. N., R. Takigiku, J. Hayes, J. W. Louda, and E. W. Baker (1989), The post-Paleozoic chronology and mechanism of ^{13}C depletion in primary marine organic matter, *Am. J. Sci.*, *289*, 436–454.

Pratt, L. M. (1984), Influence of paleoenvironmental factors on the preservation of organic matter in middle Cretaceous Greenhorn Formation near Pueblo, Colorado, *Am. Assoc. Pet. Geol. Bull.*, *68*, 1146–1159.

Pratt, L. M., and L. K. Barlow (1985), Isotopic and sedimentalogical study of the lower Niobrara Formation, Lyons, Colorado, in *Fine-Grained Deposits and Biofacies of the Cretaceous Western Interior Seaway: Evidence of Cyclic Sedimentary Processes. Society of Economic Paleontology and Mineralogy Field Trip Guidebook*, vol. 4, pp. 288, SEPM, Denver, Colo.

Pratt, L. M., M. A. Arthur, W. E. Dean, and P. A. Scholle (1993), Paleo-oceanographic Cycles and Events during the Late Cretaceous in the Western Interior Seaway of North America, in *Evolution of the Western Interior Basin*, *GAC Spec. Pap.*, edited by W. G. E. Caldwell and E. G. Kauffman, pp. 333–354, Geol. Assoc. of Canada, Toronto.

Purdue, E. M., and J. F. Koprivnjak (2007), Using the C/N ratio to estimate terrigenous inputs of organic matter to aquatic environments, *Estuarine Coastal Shelf Sci.*, *73*, 65–72.

Retallack, G. J. (2009), Greenhouse crises of the past 300 million years, *Geol. Soc. Am. Bull.*, *121*(9–10), 1441–1455.

Roberts, L. N., and M. A. Kirschbaum (1995), *Paleogeography and the Late Cretaceous of the Western Interior of Middle North America; Coal Distribution and Sediment Accumulation*, Professional Paper, vol. 1561, edited by United States Geological Society, pp. 115, USGS, Denver, Colo.

Royer, D. L., R. A. Berner, and D. J. Beerling (2001), Phanerozoic atmospheric CO_2 change: Evaluating geochemical and paleobiological approaches, *Earth Sci. Rev.*, *54*(4), 349–392.

Sageman, B. B. (1989), The benthic boundary biofacies model: Hartland Shale Member, Greenhorn Formation (Cenomanian), Western Interior, North America, *Palaeogeogr. Palaeoclimatol. Palaeoecol.*, *74*, 87–110.

Sageman, B. B., and C. Bina (1997), Diversity and species abundance patterns in Late Cenomanian black shale biofacies, Western Interior, U.S, *Palaios*, *12*, 449–466.

Sageman, B. B., and T. W. Lyons (2003), Geochemistry of fine-grained sediments and sedimentary rocks, in *Treatise on Geochemistry*, edited by F. MacKenzie, pp. 115–158, Elsevier, Oxford.

Sageman, B. B., S. R. Meyers, and M. A. Arthur (2006), Orbital time scale and new C-isotope record for Cenomanian-Turonian boundary stratotype, *Geology*, *34*(2), 125–128.

Sageman, B. B., B. S. Singer, S. R. Meyers, S. E. Siewert, I. Walaszczyk, D. J. Condon, B. R. Jicha, J. D. Obradovich, and D. A. Sawyer (2014), Integrating $^{40}Ar/^{39}Ar$, U-Pb, and astronomical clocks in the Cretaceous Niobrara Formation, Western Interior Basin, USA, *Geol. Soc. Am. Bull.*, *7–8*, 956–973.

Savdra, C. E. (1998), Ichnocoenoses of the Niobrara Formation: Implications for benthic oxygenation histories, in *Stratigraphy and Paleoenvironments of the Cretaceous Western Interior Seaway*, edited by W. E. Dean and M. A. Arthur, pp. 227–255, SEPM Concepts in Sedimentology and Paleontology, Tulsa, Okla.

Schink, B. (1988), Principles and limits of anaerobic degradation: Environmental and technological aspects, in *Biology of Anaerobic Microorganisms*, edited by A. J. B. Zehnder, pp. 771–846, John Wiley, New York.

Schlanger, S. O., and H. C. Jenkyns (1976), Cretaceous Oceanic Anoxic Events: Causes and consequences, *Geol. Mijnbouw*, *55*(3–4), 179–184.

Schlanger, S. O., M. A. Arthur, H. C. Jenkyns, and P. A. Scholle (1987), The Cenomanian-Turonian Oceanic Anoxic Event, I. Stratigraphy and distribution of organic carbon-rich beds and the marine $\delta^{13}C$ excursion, *Geol. Soc. London, Spec. Publ.*, *26*(1), 371–399.

Scott, C., and T. W. Lyons (2012), Contrasting molybdenum cycling and isotopic properties in euxinic versus non-euxinic sediments and sedimentary rocks: Refining the paleoproxies, *Chem. Geol.*, *324*, 19–27.

Scott, G. R., and W. A. Cobban (1964), Stratigraphy of the Niobrara Formation at Pueblo, Colorado, *U.S. Geol. Surv. Prof. Pap.*, *454-L*, L1–L30.

Snow, L. J., R. A. Duncan, and T. J. Bralower (2005), Trace element abundances in the Rock Canyon Anticline, Pueblo, Colorado, marine sedimentary section and their relationship to Caribbean plateau construction and oxygen anoxic event 2, *Paleoceanography*, *20*, PA3005, doi:10.1029/2004PA001093.

Taylor, S. R., and M. S. McLennan (1985), *The Continental Crust: Its Composition and Evolution*, pp. 312, Blackwell Scientific Publication, Carlton.

Tourtelot, H. A., and R. O. Rye (1969), Distribution of oxygen and carbon isotopes in fossils of Late Cretaceous age western interior region of North America, *Geol. Soc. Am. Bull.*, *80*(10), 1903–1922.

Tsandev, I., and C. P. Slomp (2009), Modeling phosphorus cycling and carbon burial during Cretaceous Oceanic Anoxic Events, *Earth Planet. Sci. Lett.*, *286*(1), 71–79.

Tsikos, H., et al. (2004), Carbon-isotope stratigraphy recorded by the Cenomanian-Turonian oceanic anoxic event: Correlation and implications based on three key-localities, *J. Geol. Soc.*, *161*, 711–720.

Turgeon, S. C., and R. A. Creaser (2008), Cretaceous Anoxic Event 2 triggered by a massive magmatic episode, *Nature*, *454*, 323–326.

Tyson, R. V., and T. H. Pearson (1991), Modern and ancient continental shelf anoxia: An overview, in *Modern and Ancient Continental Shelf Anoxia*, edited by R. V. Tyson and T. H. Pearson, pp. 1–24, Geological Society, London.

Van Mooy, B. A. S., R. G. Keil, and A. H. Devol (2002), Impact of suboxia on sinking particulate organic carbon: Enhanced carbon flux and preferential degradation of amino acids via denitrification, *Geochim. Cosmochim. Acta*, *66*, 457–465.

Wagner, T., J. S. S. Damste, P. Hofmann, and B. Beckmann (2004), Euxinia and primary production in Late Cretaceous eastern equatorial Atlantic surface waters fostered orbitally driven formation of marine black shales, *Paleoceanography*, *19*, PA3009, doi:10.1029/2003PA000898.

Wagreich, M. (2012), "OAE 3"-regional Atlantic organic carbon burial during the Coniacian-Santonian, *Clim. Past*, *8*, 1447–1455.

Walaszczyk, I., and W. A. Cobban (2000), Inoceramid faunas and biostratigraphy of the Upper Turonian-Lower Coniacian of the Western Interior of the United States, *Spec. Pap. Palaeontol.*, *64*, 1–118.

Walaszczyk, I., and W. A. Cobban (2006), Palaeontology and biostratigraphy of the Middle-Upper Coniacian and Santonian inoceramids of the US Western Interior, *Acta Geol. Pol.*, *56*(3), 241–348.

Walaszczyk, I., and W. A. Cobban (2007), Inoceramid fauna and biostratigraphy of the upper Middle Coniacian-lower Middle Santonian of the Pueblo Section (SE Colorado, US Western Interior), *Cretaceous Res.*, *28*(1), 132–142.

Walaszczyk, I., J. A. Shank, A. G. Plint, and W. A. Cobban (2014), Interregional correlation of disconformities in Upper Cretaceous strata, Western Interior Seaway: Biostratigraphic and sequence-stratigraphic evidence for eustatic change, *Geol. Soc. Am. Bull.*, *126*(3–4), 307–316.

Watkins, D. K. (1989), Nannoplankton productivity fluctuations and rhythmically-bedded pelagic carbonates of the Greenhorn Limestone (Upper Cretaceous), *Palaeogeogr. Palaeoclimatol. Palaeoecol.*, *74*, 75–86.

Wendler, I. (2013), A critical evaluation of carbon isotope stratigraphy and biostratigraphic implications for Late Cretaceous global correlation, *Earth Sci. Rev.*, *126*, 116–146.

White, T., and M. A. Arthur (2006), Organic carbon production and preservation in response to sea-level changes in the Turonian Carlile Formation, US Western Interior Basin, *Palaeogeogr. Palaeoclimatol. Palaeoecol.*, *235*(1), 223–244.

Wright, E. K. (1987), Stratification and paleocirculation of the Late Cretaceous Western Interior Seaway of North America, *Geol. Soc. Am. Bull.*, *99*(4), 480–490.

Zonneveld, K. A. F., et al. (2010), Selective preservation of organic matter in marine environments; processes and impact on the sedimentary record, *Biogeosciences*, *7*, 483–511.